PROCEEDINGS OF SCIENCE

Precision measurements with kaons at CERN

Letizia Peruzzo[1,*]

Johannes Gutenberg Universität Mainz Institut für Physik and PRISMA$^+$ Cluster of Excellence, Staudingerweg 7, Mainz 55128, Germany.

E-mail: letizia.peruzzo@cern.ch

The NA62 experiment at CERN collected the world's largest data set of charged kaon decays in 2016-2018 (Run1), leading to the first measurement of the branching ratio of the ultra-rare $K^+ \to \pi^+\nu\bar{\nu}$ decay. An overview of the latest NA62 results on precision measurements based on Run1 data is presented. An analysis of the flavor-changing neutral current $K^+ \to \pi^+\mu^+\mu^-$ decay, based on about 28×10^3 signal events with negligible background contamination, leads to the most precise determination of the branching ratio and of the form factor. The radiative kaon decay $K^+ \to \pi^o e^+\nu\gamma$ ($K_{e3\gamma}$) is studied with a data sample of $O(10^5)$ $K_{e3\gamma}$ candidates with sub-percent background contamination. The most precise measurements of the branching ratio and T-asymmetry are achieved. New preliminary results are obtained from an analysis of the $K^+ \to \pi^+\gamma\gamma$ decay using data collected with a minimum-bias trigger. The sample, about 15 times larger than the previous largest one, leads to an unprecedented sensitivity.

8th Symposium on Prospects in the Physics of Discrete Symmetries (DISCRETE 2022)
7-11 November, 2022
Baden-Baden, Germany

*Speaker
[1]On behalf of the NA62 Collaboration.

PoS(DISCRETE2022)070

1. The NA62 experiment

The NA62 experiment is the latest in a series of fixed-target experiments located at the CERN SPS using the decay-in-flight technique to explore kaon decays. The experiment aims to precisely measure the branching ratio of the very rare decay $K^+ \to \pi^+ \nu\bar{\nu}$ with at least 20% accuracy, collecting up to 100 events in a few years of data taking. About 4×10^{12} kaon decays were collected during the data-taking period 2016-2018 (referred to as NA62 Run1) and the result of the corresponding branching ratio (BR) measurement is $\mathrm{BR}(K^+ \to \pi^+ \nu\bar{\nu}) = (10.6 \pm 4.0) \times 10^{-11}$ [1]. Moreover, NA62 serves as a multi-purpose experiment covering a broad kaon and beam-dump physics program. A detailed description of the experiment can be found in [2].

NA62 uses the SPS proton beam (400 GeV/c momentum), which hits on a beryllium target and produces a secondary hadron beam, with kaons contributing to 6% of all particles. The beam has a momentum of (75 ± 1) GeV/c and a nominal intensity of 750 MHz. The detector apparatus (Figure 1) extends over 270 m from the target to the end of the experiment. Kaon tagging and a

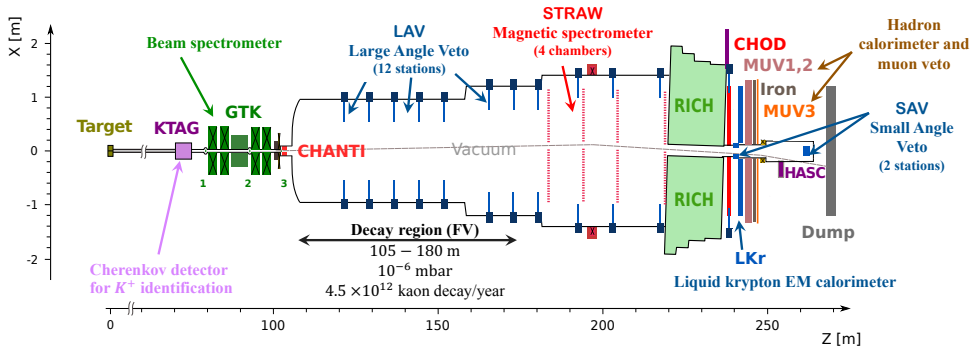

Figure 1: Schematic layout of the NA62 experiment in the X-Z plane.

precise timing measurement of the beam particles are provided by a Cherenkov detector (KTAG), followed by three silicon pixel stations which form the beam spectrometer (Gigatracker or GTK). A magnetic spectrometer of four STRAW chambers placed in vacuum provides the momenta and directions of the charged particles produced in the kaon decays. The particle identification is performed by a Ring Imaging Cherenkov (RICH) detector, an electromagnetic (LKr) calorimeter, a hadron calorimeter of two modules (MUV1 and MUV2) and a muon counter (MUV3). A Large Angle (LAV) and a Small Angle (SAV) Veto form together with the LKr calorimeter the high-efficiency photon-veto system, covering angles from 0 to 50 mrad. A pair of charged hodoscopes (CHOD) provide the timing for the tracks of the final state particles. The experimental setup is completed by a scintillator detector (CHANTI) and a hadron calorimeter (HASC) to reduce critical background induced by inelastic interactions of the beam with the final collimator and the GTK, and background from kaon decays with particle products traveling along the beam line. The overall time resolution of the experiment reaches $O(100)$ ps and the detectors have to stand a rate of about 10 MHz of events. For these purposes high-performance read-out and trigger systems have been developed [3, 4].

2. $K^+ \to \pi^+\mu^+\mu^-$ decay

This section reports the results of the analysis of the decay $K^+ \to \pi^+\mu^+\mu^-$, based on data collected by NA62 in 2017-2018 [5]. Flavor-changing-neutral current processes $K^\pm \to \pi^\pm\ell^+\ell^-$ ($K_{\pi\ell\ell}$) [6] are dominated by virtual photon exchange $K^\pm \to \pi^\pm\gamma^* \to \pi^\pm\ell^+\ell^-$ and involve long-distance hadronic effects described by a vector interaction form factor. This is a complex function usually denoted as $W(z)$ with z being the normalized di-lepton squared invariant mass $z = m^2_{\ell\ell}/m^2_K$. The presented analysis involves the parametrization of $W(z)$ as described in the framework of Chiral Perturbation Theory (ChPT) at $O(p^6)$ order [7]

$$W(z) = G_F m_K^2\,(a_+ + b_+ z) + W^{\pi\pi}(z), \tag{1}$$

where a_+ and b_+ are real parameters, and $W^{\pi\pi}$ is a complex function describing the contribution from a two-pion loop. [1]

Events with three charged particles in the final state, each satisfying particle identification criteria, are selected in the signal sample. The 3-body decay $K^+ \to \pi^+\pi^+\pi^-$ is used as normalization channel and provides the number of kaon decays available in this analysis, $N_K \approx 3.5 \times 10^{12}$. The reconstructed mass spectrum of the selected events in the signal sample is shown in the left panel of Figure 2 for both data and simulation. In the $m_{\pi\mu\mu}$ signal region 27 679 data events are selected

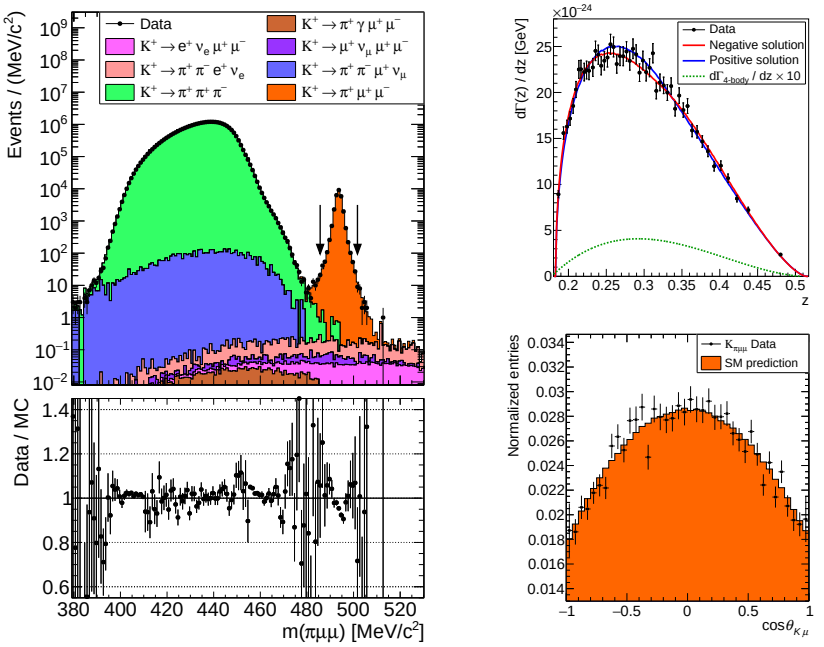

Figure 2: Left: Reconstructed mass distribution of events satisfying the signal selection. The contribution from the simulated $K_{\pi\mu\mu}$ decay is scaled according to the PDG [9] branching ratio. Arrows indicate the selected mass region. **Top Right:** Reconstructed $K_{\pi\mu\mu}$ differential decay width. The superimposed colored lines correspond to the form factor fit solutions. **Bottom Right:** Reconstructed $\cos\theta_{K\mu}$ spectrum from data (point with error bars), and the distribution expected from the Standard Model (histogram). Figure from [5].

[1] The $W^{\pi\pi}$ term depends itself on external parameters. For the presented analysis the values of [8] are used.

with a background contamination, based on simulation, of 8 events. The reconstructed differential decay width is plotted in 50 equipopulated bins in z with widths ranging from 0.004 for $z \approx 0.25$ to 0.066 for the last bin, as shown in the top right panel of Figure 2. By a simple integration over z of the differential decay width spectrum and a multiplication by $\tau_K/\hbar$, the model-independent branching ratio is obtained

$$\mathrm{BR}(K^+ \to \pi^+\mu^+\mu^-) = (9.15 \pm 0.08) \times 10^{-8} \tag{2}$$

which is consistent with previous measurements but at least a factor three more precise as shown in Figure 3 left panel. The form factor parameters a_+ and b_+, best describing the data, are determined by a χ^2 fit of the differential decay width data points. The theoretically-preferred [10] *negative solution* (with both parameters negative) is

$$a_+ = -0.575 \pm 0.013 \text{ and } b_+ = -0.722 \pm 0.043 \tag{3}$$

in agreement with results form previous experiments both in muon and electron mode as expected by lepton-flavor universality in $K_{\pi\ell\ell}$ decays, Figure 3 right panel. The forward-backward asymmetry

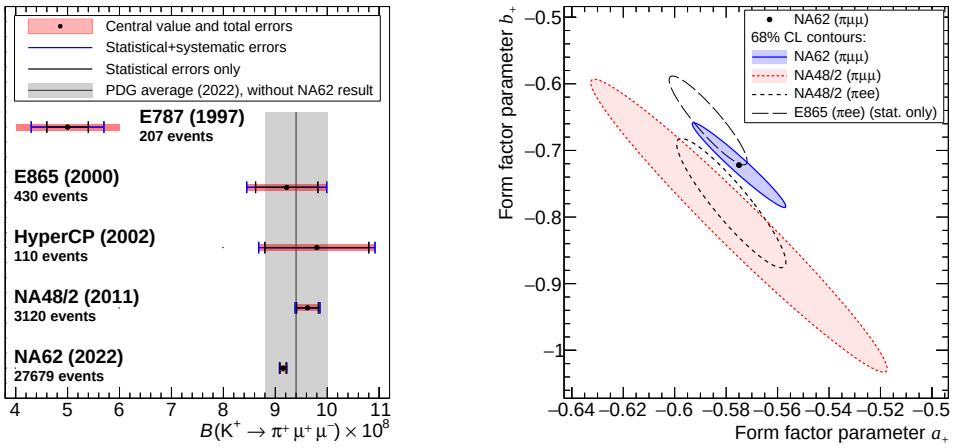

Figure 3: Comparison with earlier measurements. **Left:** $K_{\pi\mu\mu}$ branching ratio, with the PDG [9] average as a shaded band. **Right:** Combined statistical and systematic 68% confidence level (CL) contours in the (a_+, b_+) plane for the muon and electron modes. Figure from [5].

A_{FB} of the decay is defined in terms of the angle $\theta_{K\mu}$ between the K^+ and the μ^- three-momenta in the di-muon rest frame. The resulting distribution of $\cos\theta_{K\mu}$ is shown in the bottom right panel of Figure 2. The asymmetry is measured to be

$$A_{\mathrm{FB}} = (0.0 \pm 0.7) \times 10^{-2} \tag{4}$$

with no significant dependency over z and the statistical precision being for the first time at the level of the upper limits predicted by the theory [11].

3. $K^+ \to \pi^o e^+ \nu\gamma$ decay

This section reports the preliminary results on the measurement of the branching ratio and of T-violation for the process $K^+ \to \pi^o e^+ \nu\gamma$ [12], based on data collected by NA62 in 2017 and 2018.

The $K^+ \to \pi^o e^+ \nu\gamma$ ($K_{e3\gamma}$) decay is well described in the ChPT framework. The branching ratio is usually normalized to that of $K^+ \to \pi^o e^+ \nu$ (K_{e3}) as

$$R_j = \frac{\mathrm{BR}(K^j_{e3\gamma})}{\mathrm{BR}(K_{e3})} = \frac{\mathrm{BR}(K^+ \to \pi^o e^+ \nu\gamma \mid E^j_\gamma, \theta^j_{e,\gamma})}{\mathrm{BR}(K^+ \to \pi^o e^+ \nu(\gamma))} \tag{5}$$

where E^j_γ and $\theta^j_{e,\gamma}$ represent restrictions to the phase space in terms of the radiative photon energy E^j_γ and the angle $\theta^j_{e,\gamma}$ between the radiative photon and the charged lepton, due to the divergent decay amplitude for $E_\gamma \to 0$ and $\theta_{e,\gamma} \to 0$. The most commonly used definitions for the R_j kinematic regions in the kaon rest frame are given in Table 1, together with the corresponding theoretical expectation from ChPT calculations [13] and recent experimental results. Possible T-violation

R region	E_γ	$\theta_{e,\gamma}$	$O(p^6)$ **ChPT** $R_j \times 10^2$	**ISTRA+** $R_j \times 10^2$	**OKA** $R_j \times 10^2$
$R1$	$E_\gamma > 10$ MeV	$\theta_{e,\gamma} > 10^\circ$	1.804 ± 0.021	$1.81 \pm 0.03 \pm 0.07$	$1.990 \pm 0.017 \pm 0.021$
$R2$	$E_\gamma > 30$ MeV	$\theta_{e,\gamma} > 20^\circ$	0.640 ± 0.008	$0.63 \pm 0.02 \pm 0.03$	$0.587 \pm 0.010 \pm 0.015$
$R3$	$E_\gamma > 10$ MeV	$0.6 < \cos\theta_{e,\gamma} < 0.9$	0.559 ± 0.006	$0.47 \pm 0.02 \pm 0.03$	$0.532 \pm 0.010 \pm 0.012$

Table 1: R_j definitions in terms of E_γ and the $\theta_{e,\gamma}$ in the kaon rest frame, and respective expectations from ChPT $O(p^6)$ order calculations [13] and results of the measurements performed by the ISTRA+ [14] and the OKA [15] experiments.

effects in the $K_{e3\gamma}$ decay can be studied through the T-odd observable ξ and the corresponding asymmetry A_ξ

$$\xi = \frac{\overrightarrow{p_\gamma} \cdot (\overrightarrow{p_e} \times \overrightarrow{p_\pi})}{m_K^3}, \tag{6}$$

where $\overrightarrow{p_i}$ is the reconstructed 3-momentum of the i particle and m_K the kaon mass. Different theoretical, Standard Model and beyond, calculations of A_ξ [16] give values in the range $[-10^{-4}, -10^{-5}]$ while the current experimental sensitivity is two orders of magnitude worse and refers only to the kinematic region R_3 [14]: $A_\xi^{\mathrm{ISTRA+}}(R_3) = (1.5 \pm 2.1) \times 10^{-2}$.

Experimentally the normalized branching ratio R_j is determined as

$$R_j = \frac{\mathrm{BR}(K^j_{e3\gamma})}{\mathrm{BR}(K_{e3})} = \frac{N^{\mathrm{obs}}_{K^j e3\gamma} - N^{\mathrm{bkg}}_{K^j e3\gamma}}{N^{\mathrm{obs}}_{Ke3} - N^{\mathrm{bkg}}_{Ke3}} \cdot \frac{A_{Ke3}}{A_{K^j e3\gamma}} \cdot \frac{\varepsilon^{\mathrm{trig}}_{Ke3}}{\varepsilon^{\mathrm{trig}}_{K^j e3\gamma}} \tag{7}$$

where $N^{\mathrm{obs}}_{Ke3\gamma(Ke3)}$ and $N^{\mathrm{bkg}}_{Ke3\gamma(Ke3)}$ are the numbers of observed and expected background events in the signal (normalization) sample, $A_{Ke3\gamma(Ke3)}$ is the acceptance measured with simulations, and $\varepsilon^{\mathrm{trig}}_{Ke3\gamma(Ke3)}$ is the trigger efficiency from data for the signal (normalization) sample. [2] For the normalization channel about 66×10^6 events are selected, while for the signal about 130×10^3, 54×10^3 and 39×10^3 events are selected in the R_1, R_2 and R_3 regions. Figure 4 shows the distributions of the missing mass parameter $m^2_{\mathrm{miss}} = (P_K - P_e - P_{\pi^o} - P_\gamma)^2$, where P_{particle} are the 4-momenta of the reconstructed particles, for the selected events. In the signal regions the main

[2] Note that the only difference between signal and normalization selections is the treatment of the third photon in the event, ensuring a first-order cancellation of several systematic effects.

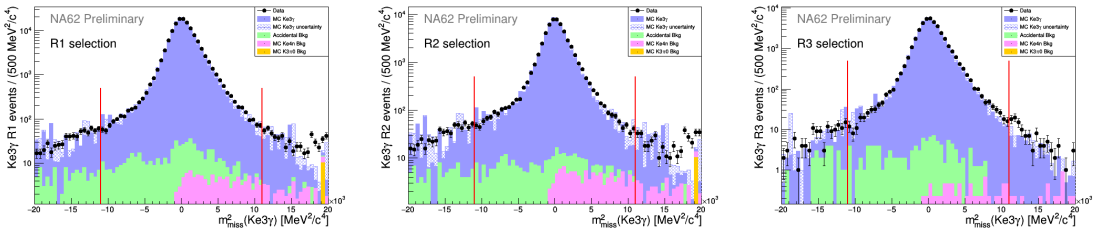

Figure 4: $m^2_{\rm miss}$ distributions for selected $K_{e3\gamma}$ events in data (black dots) compared with the expected signal and all the background sources (histograms). The signal regions are enclosed in the red lines.

background contamination arises from $K^+ \to \pi^o e^+ \nu$ events with one more LKr cluster, coming from accidental activity, that mimics the radiative photon (accidental background). Its contamination in the signal samples is measured from data with out-of-time sidebands. The ratio between expected background and signal events is below 1% in all three R_j regions. The preliminary results of the measurements of R_j and of the T-asymmetry A_ξ are reported in Table 2. The precision of the R_j

***R* region**	***R* value**	**A_ξ value**
R_1	$(1.684 \pm 0.005 \pm 0.010) \times 10^{-2}$	$-0.001 \pm 0.003 \pm 0.002$
R_2	$(0.559 \pm 0.003 \pm 0.005) \times 10^{-2}$	$-0.003 \pm 0.004 \pm 0.003$
R_3	$(0.523 \pm 0.003 \pm 0.003) \times 10^{-2}$	$-0.009 \pm 0.005 \pm 0.004$

Table 2: Preliminary results for the value of the R parameter and T-asymmetry A_ξ in the three kinematic regions of the phase space as defined in Table 1.

preliminary results is improved by a factor between 2 and 3 with respect to the state of the art. For the T-asymmetry the preliminary results represent upper limits since they are compatible with absence of T-violation. However, the preliminary measurement in R_3 improves by a factor 3 in term of precision the most recent experimental result, and the two other represent the first preliminary measurements ever performed for these physical quantities.

4. $K^+ \to \pi^+\gamma\gamma$ decay

This section reports the preliminary results on the $K^+ \to \pi^+\gamma\gamma$ analysis [17], performed using the full Run1 data set collected by NA62. The $K^+ \to \pi^+\gamma\gamma$ decay represents a crucial test on the precision of the ChPT to describe weak processes at low energy. At the leading $O(p^4)$ order, and including next-to-leading $O(p^6)$ order contribution, the decay rate and spectrum are determined by a single *a priori* unknown $O(1)$ parameter $\hat{c}$ [18]. The total decay rate is predicted to be $\mathrm{BR}(K^+ \to \pi^+\gamma\gamma) \sim 10^{-6}$, and the spectrum presents a characteristic cusp for a value of the di-photon invariant mass equal to twice the charged pion mass. The decay spectrum is usually given in terms of the parameter $z = m^2_{\gamma\gamma}/m^2_K$, where $m_{\gamma\gamma}$ and m_K are the invariant di-photon and the kaon masses, respectively, as shown in Figure 5 left panel.

The analysis is performed for value of $z > 0.25$ after reconstructing the full final state of the kaon decay. About 4×10^3 events are observed with 393 ± 20 expected background events. Two main sources of background are identified: i) $K^+ \to \pi^+\pi^o\pi^o$ events where two photons from the

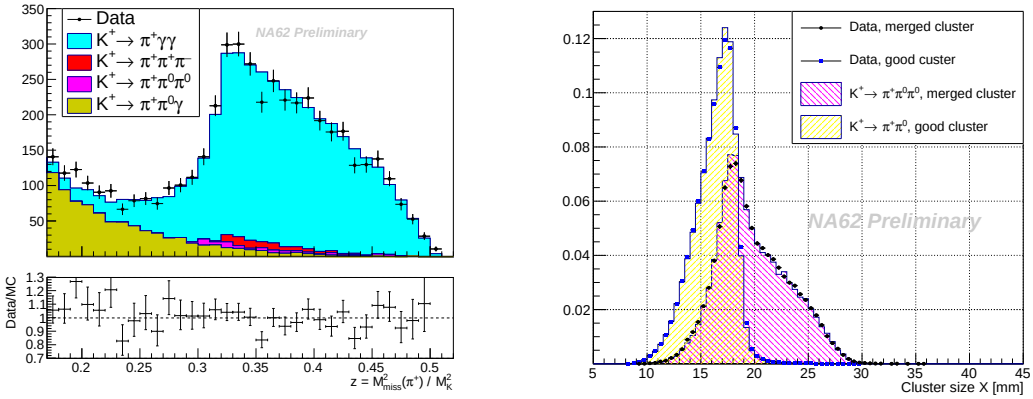

Figure 5: Left: Reconstructed $z = m^2_{\gamma\gamma}/m^2_K$ spectrum for data compared to estimated signal and background components. The signal region is defined for $z > 0.25$. **Right:** X size of the reconstructed cluster in the LKr electromagnetic calorimeter. Events with merged clusters exhibits a bump for X dimension above 20 mm.

π^os merged in a single cluster in the LKr calorimeter, and ii) $K^+ \to \pi^+\pi^+\pi^-$ events where two tracks are out of acceptance of the STRAW spectrometer. The validation of the background estimation is performed looking at the data/simulation agreement in control regions with enhanced background events. Figure 5 right shows the cut applied to reduce the type i) background. From a likelihood fit to the data z spectrum the value of the $\hat{c}$ parameter is obtained together with the corresponding branching ratio

$$\hat{c} = 1.713 \pm 0.084 \text{ and } \mathrm{BR}(K^+ \to \pi^+\gamma\gamma) = (9.73 \pm 0.19) \times 10^{-7}. \quad (8)$$

This preliminary results improve on the best previous measurements as shown in Figure 6 and the total uncertainty is reduced by a factor 3. The analysis can also be re-interpreted as a search for new-physics particles decaying to two photons in the channel $K^+ \to \pi^+ X, X \to \gamma\gamma$.

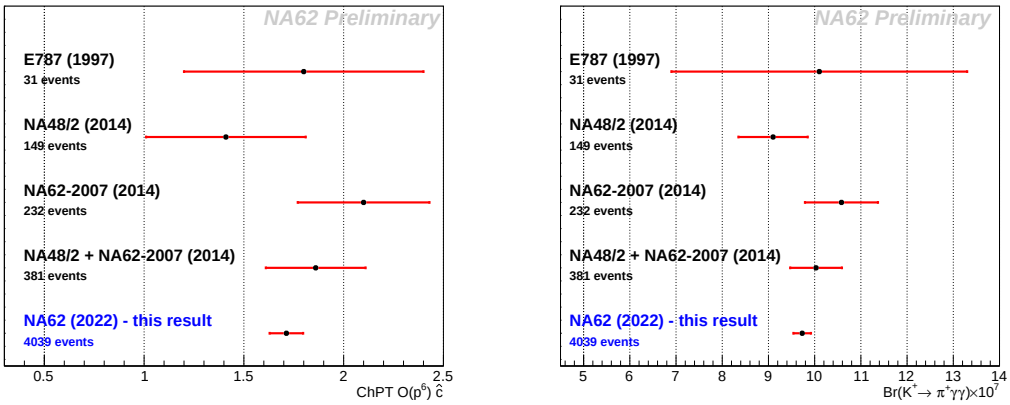

Figure 6: Comparison with early measurements. **Left:** $\hat{c}$ parameter at $O(p^6)$ order in the framework of ChPT. **Right:** $K^+ \to \pi^+\gamma\gamma$ branching ratio.

5. Conclusions and outlook

NA62 successfully completed the data-taking period in 2016-2018. Results of various analysis performed on Run1 data have been presented. NA62 Run2 started in spring 2021, following detector and trigger upgrades, and it is approved until the Long Shutdown 3 (LS3) at CERN, foreseen at the end of 2025. A long-term kaon decay program at CERN High Intensity Kaon Experiment (HIKE) has been proposed [19].

References

[1] E. Cortina Gil *et al* [NA62 Collaboration], *JHEP* **06** (2021) 093.

[2] E. Cortina Gil *et al* [NA62 Collaboration], *JINST* **12** (2017) P05025.

[3] R. Ammendola *et al*, *Nucl. Instrum. Meth.* A **929** (2019) 1.

[4] The NA62 Collaboration, *submitted to JHEP*, [hep-ex:2208.00897].

[5] E. Cortina Gil *et al* [NA62 Collaboration], *JHEP* **11** (2022) 011.

[6] G. Ecker, A. Pich and E. de Rafael, *Nucl. Phys. B* **291** (1987) 692.
A. Z. Dubnickova *et al*, *Phys. Part. Nucl. Lett.* **5** (2008) 76.
B. Kubis and R. Schmidt, *Eur. Phys. J. C* **70** (2010) 219.

[7] G. D'Ambrosio *et al*, *JHEP* **08** (1998) 004.

[8] G. D'Ambrosio *et al*, *Phys. Lett. B* **835** (2022) 137594.

[9] R. L. Workman *et al* [Particle Data Group], *Prog. Theor. Exp. Phys.* **2022** (2022) 083C01.

[10] G. D'Ambrosio, D. Greynat and M. Knecht, *JHEP* **02** (2019) 49.

[11] C.-H. Chen, C.Q. Geng and I.-L. Ho, *Phys. Rev. D* **67** (2003) 074029.
D.-N. Gao, *Phys. Rev. D* **69** (2004) 094030.

[12] *Paper in preparation*.

[13] B. Kubis *et al*, *Eur. Phys. J. C* **50** (2007) 557-571.

[14] S. A. Akimenko *et al* [ISTRA+ Collaboration], *Phys. Atom. Nuclei* **70** (2007) 702.

[15] A. Y. Polyarush *et al* [OKA Collaboration], *Eur. Phys. J. C* **81** (2021) 161.

[16] E. Müller, B. Kubis and UG. Meißner, *Eur. Phys, J. C* **48** (2006) 427.
V. V. Braguta, A. A. Likhoded and A. E. Chalov, *Phys. Rev. D* **68** (2003) 094008.

[17] *Paper in preparation*.

[18] G. D'Ambrosio and J. Portolés, *Phys. Lett. B* **386** (1996) 403.

[19] E. Cortina Gil *et al* [HIKE Collaboration], [hep-ex:2211.16586].